

(NASA-CR-161516) EVALUATION OF SPACE  
SHUTTLE MAIN ENGINE BEARINGS FROM HIGH  
PRESSURE OXYGEN TURBOPUMP 9008 Final Report  
(Battelle Columbus Labs., Ohio.) 32 p  
HC A03/MF A01

N80- 28426

Unclassified  
CSCL 21H G3/20 28172

REPRODUCED BY  
**NATIONAL TECHNICAL  
INFORMATION SERVICE**  
U.S. DEPARTMENT OF COMMERCE  
SPRINGFIELD, VA. 22161

FINAL REPORT

on

EVALUATION OF SPACE SHUTTLE MAIN ENGINE BEARINGS  
FROM HIGH PRESSURE OXYGEN TURBOPUMP 9008  
(Contract No. NAS8-33576 - Task No. 102)

to

NATIONAL AERONAUTICS AND SPACE ADMINISTRATION  
GEORGE C. MARSHALL SPACE FLIGHT CENTER

by

K.F. Dufrane and J.W. Kannel

July 11, 1980

BATTELLE  
COLUMBUS LABORATORIES  
505 KING AVENUE  
COLUMBUS, OHIO 43201

TABLE OF CONTENTS

	<u>Page</u>
INTRODUCTION. . . . .	1
SUMMARY AND RECOMMENDATIONS . . . . .	2
COMPONENT INSPECTION. . . . .	3
Bearing S/N 9519531. . . . .	3
Bearing S/N 8549515. . . . .	15
LOAD AND STRESS ANALYSIS. . . . .	18
General Approach . . . . .	18
Inputs for Bearing Load Calculations . . . . .	22
Estimation of Actual Loads and Fatigue Lives . . . . .	22
Measuring Units. . . . .	28

LIST OF FIGURES

Figure 1. Ball-Path Spalling and Chipping at Edge of Race Curvature on Bearing S/N 8519531 . . . . .	4
Figure 2. Profile of Burr at Edge of Race Curvature on Inner Race of Bearing S/N 8519531. . . . .	5
Figure 3. Inner Race Cross-Race Curvature Taken at Positions 180 Degrees Apart on Bearing S/N 8549531 . . . . .	7
Figure 4. Outer Race Cross-Race Curvature and Typical Non-Spalled Ball Roundness from Bearing S/N 8549531 . . . . .	8
Figure 5. Scanning Electron Micrographs of Surface Spalling on Inner Race of Bearing S/N 8519531. . . . .	9
Figure 6. Spalling on Ball and Outer Race Surfaces of Bearing S/N 8519531 . . . . .	10
Figure 7. Subsurface Cracking on Races of Bearing S/N 8519531 . . . . .	12

LIST OF FIGURES  
(CONTINUED)

	<u>Page</u>
Figure 8. Oxide in Subsurface Cracks on Races of Bearing S/N 8519531. . . . .	13
Figure 9. Ball Pocket Elongated by Wear in Retainer from Bearing S/N 8519531 . . . . .	16
Figure 10. Inner Race Cross-Race Curvatures Taken at Positions 180 Degrees Apart on Bearing S/N 8549515. . . . .	19
Figure 11. Outer Race Cross-Race Curvature and Typical Ball Roundness from Bearing 8549515. . . . .	20
Figure 12. Location of Measured Ball Contact Paths on Bearing S/N 8549531. . . . .	23
Figure 13. Location of Measured Ball Contact Paths on Bearing S/N 8549531. . . . .	24
Figure 14. Location of Measured Ball Contact Paths on Bearing S/N 8549515. . . . .	25

LIST OF TABLES

Table 1. Microhardness Readings Taken Across Region of Subsurface Cracks on Races of Bearing S/N 95319531. . . . .	14
Table 2. Ball Pocket Dimensions on Retainer from Bearing S/N 8519531. . . . .	17
Table 3. Summary of Bearing Stress Computations . . . . .	27

EVALUATION OF SPACE SHUTTLE MAIN ENGINE BEARINGS  
FROM HIGH PRESSURE OXYGEN TURBOPUMP 9008

by

K.F. Dufrane and J.W. Kannel

INTRODUCTION

NASA is currently involved in the development of long-life turbopumps for use on the shuttle. Because of the reusable design of the shuttle, lifetimes of 27,000 seconds (7.5 hours) are being sought, whereas most turbopumps to date have operated for periods of on the order of only hundreds of seconds. While all components are being considered in efforts to achieve satisfactory lifetimes, the turbopump mainshaft support bearings are of particular concern. In support of these efforts, Battelle's Columbus Laboratories (BCL) undertook a 1-month study to examine a used set of bearings and to recommend the subsequent steps needed to achieve the desired lifetimes.

The two bearings examined were run in the high pressure oxygen turbopump No. 9008 on Engine No. 2004. The bearings are angular-contact ball bearings, applied as a preloaded pair, locked to the shaft, inner race rotating, with the outer races unrestrained axially (i.e., the bearings provide radial location only). The bearings examined in the study were S/N 8549515 (Position No. 4) and S/N 8549531 (Position No. 3) from the turbine end. The engine reportedly had experienced seven starts and had run a total of 2406 seconds, of which 1090 seconds were at full power load (109 percent of speed).

Battelle's specific objectives in the study were:

- (1) Perform a visual, scanning electron microscopy (SEM), metallurgical, and dimensional analysis of the bearings  
(as needed)

- (2) Estimate the nature and magnitude of the loads applied to the bearings based on the contact patterns
- (3) Recommend further analytical efforts required and any design, material, or lubrication changes that will improve the durability of the bearings.

#### SUMMARY AND RECOMMENDATIONS

The examinations and load calculations made on the two bearings have shown that one of the bearings, S/N 8549531, had been subjected to severe overloads. The overloads resulted in extensive fatigue spalling on the races and balls and advanced retainer wear. Axial loads as high as 45,000 N (10,000 pounds) with radial loads of 8900 N (2000 pounds) were estimated.  $B_1$  fatigue life predictions corresponding to these loads are less than 100 seconds, which was confirmed by the presence of the extensive fatigue spalling. The mating bearing, S/N 8549515, was subjected to a 3200 N (850 pounds) axial load with a 8900 N (2000 pounds) radial load. Because of the unintended radial load, the  $B_1$  fatigue life prediction for it was also reduced to between 1400 and 7900 seconds as opposed to more than 20,000 seconds with intended design loads.

The high applied bearing loads leading to fatigue spalling is clear evidence of the presence of unintended high internal loads in the high pressure oxygen pump. These loads caused extensive fatigue damage to the bearing in Position No. 3 (S/N 8549531) and complete bearing failure leading to extensive secondary pump damage was almost certainly imminent.

Based upon these findings, action must be initiated to reduce the applied bearing loads to levels within the bearing tolerance capabilities (the pump design loads are reasonable to obtain the necessary life from the bearings). Alternatively, if the source of the excessive loads cannot be identified or reliably controlled, design changes must be made to incorporate a bearing of sufficient size to withstand the high loads. The repeated experience of excessive loading on bearings from the turbopumps suggests that exercising at least one of these options will be critical to attaining the reliability appropriate for a SSME turbopump.

#### COMPONENT INSPECTION

##### Bearing S/N 9519531

###### Races

The races of bearing 8519531 were both heavily spalled in the ball contact path, which indicated operation under distress. The inner race had a heavily worn and deformed region at the shoulder portion of the race surface. The edge of the race curvature was chipped, as shown in Figure 1. The edge was also plastically deformed slightly, as shown in Figure 2. The contact path on the inner race showed some evidence of a synchronous radial load combined with a high thrust loading. The heavily worn and deformed path extended from the shoulder (the chamfer was completely removed) to 3.81 mm (0.150 inch) at one extreme to 3.55 mm (0.140 inch) at the other extreme, located 180 degrees apart. Extending beyond the worn region was a band of pits varying in width from 1.40 mm (0.055 inch) to 2.54 mm (0.10 inch) with the wider portion corresponding to 3.81 mm (0.150 inch) worn portion. Superimposed on the worn region was a narrow dark band (apparently the edge of contact for some period of operation subsequent to the high-wear period). It also varied in position, from 2.92 mm (0.115 inch) to 3.68 mm (0.145 inch).

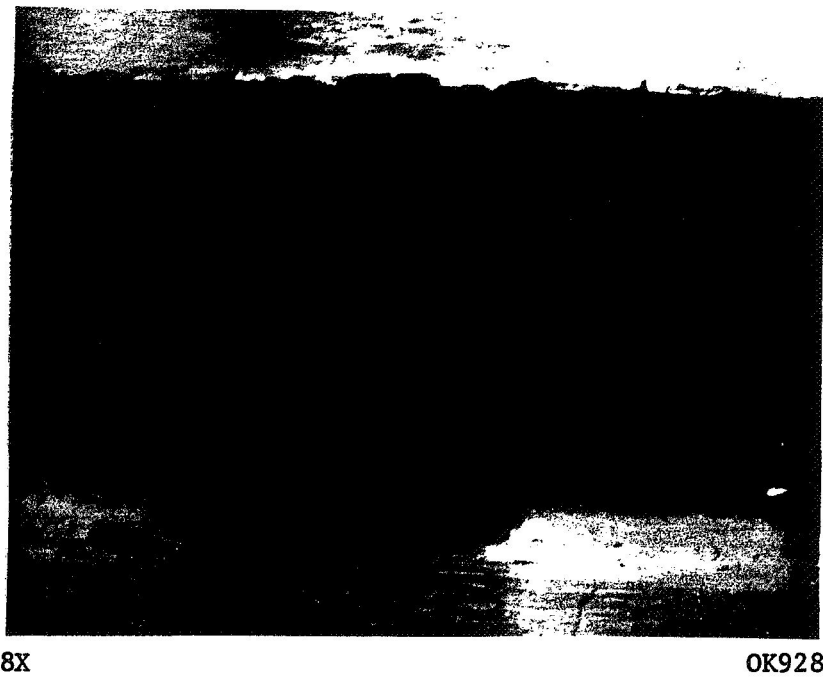


FIGURE 1. BALL-PATH SPALLING AND CHIPPING AT EDGE  
OF RACE CURVATURE ON BEARING  
S/N 8519531

ORIGINAL PAGE IS  
OF POOR QUALITY

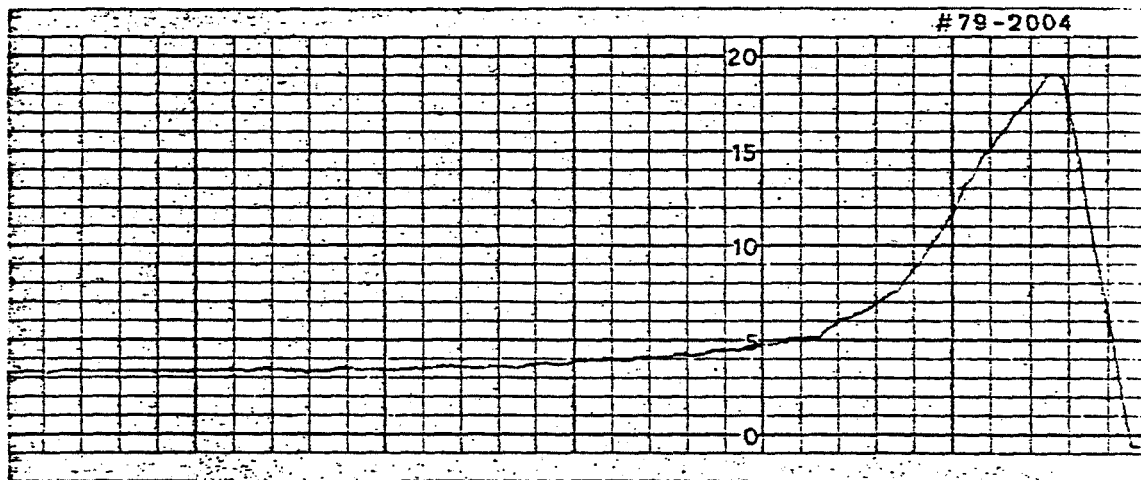


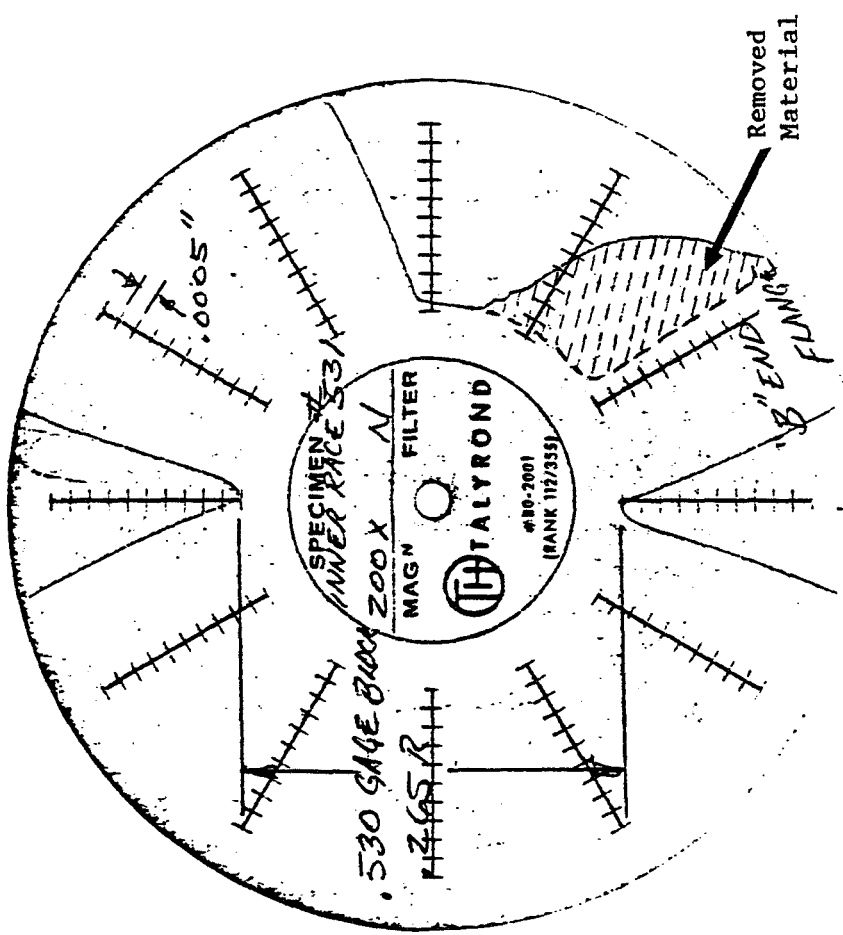
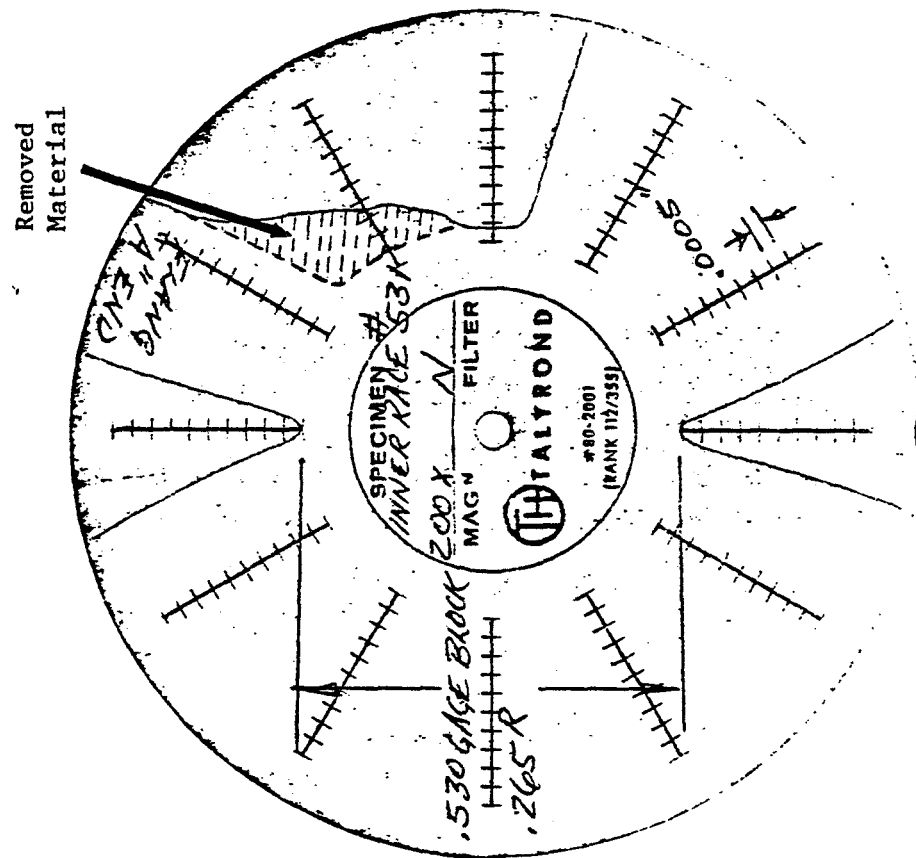
FIGURE 2. PROFILE OF BURR AT EDGE OF RACE CURVATURE ON  
INNER RACE OF BEARING S/N 8519531.  
Magnifications: Vertical, each small division =  
0.0051 mm (0.0002 inch); Horizontal, each small  
division = 0.051 mm (0.002 inch)

Cross-race curvature measurements at the extremes of the variation in track location confirmed the material removal. As shown in Figure 3, the wear depth at the shoulder varied from approximately 0.15 mm (0.006 inch) to 0.10 mm (0.004 inch). Since the burr at the edge, shown in Figure 2, does not have a volume sufficient to account for the material loss on the race, the loss occurred by wear.

The outer race also showed evidence of heavy ball contact over a major portion of the race curvature, including a band of heavy pitting. The contact paths were skewed slightly, which on the outer race is the result of misalignment and/or a fixed radial load superimposed on the axial load. At one extreme, the contact started at 0.76 mm (0.030 inch) from the chamfer and extended in a smooth worn band for 2.29 mm (0.090 inch). At the edge of this wear band was a band of heavy pitting measuring approximately 2.4 mm (0.095 inch) wide. Extending beyond the band of pits was another smoothly worn, darkened band 5.1 mm (0.200 inch) wide. In the position at 180 degrees from the above description, the other extreme in track location was located. The location of the first smoothly worn band extended to the edge of the chamfer. The band of pitting was much less severe in this location and was only 0.76 mm (0.030 inch) wide. Beyond the band of pits, the second smoothly worn band measured 6.35 mm (0.250 inch) wide. Locations of these track positions are shown graphically in Figures 6, 12, and 13, which were used to measure the contact angles as part of the load-estimate calculations.

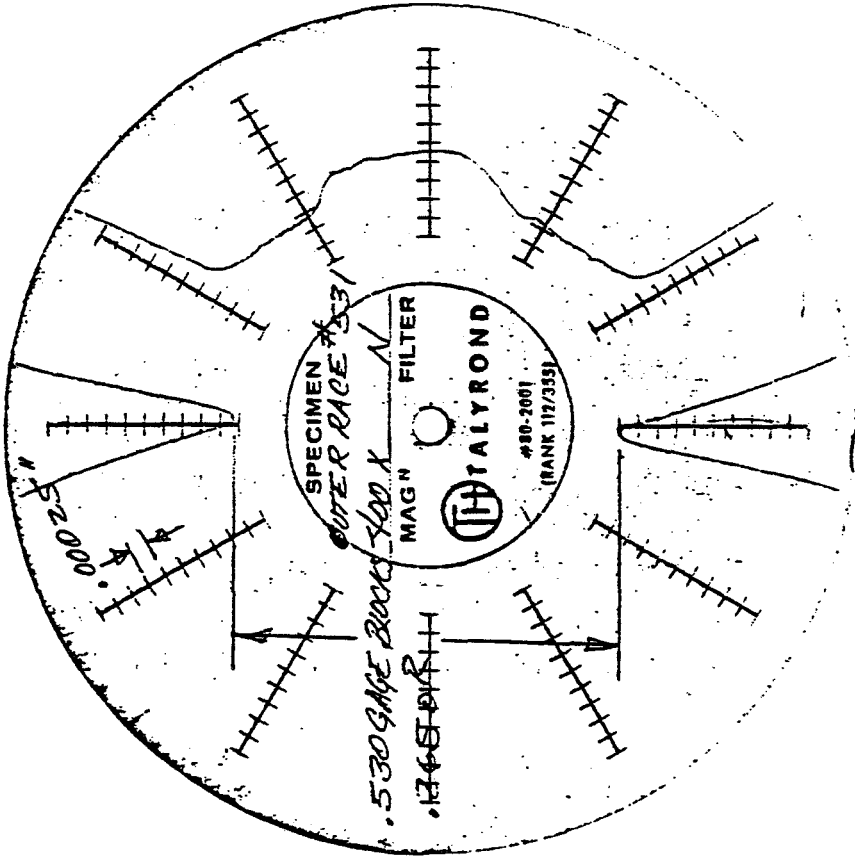
Cross-race curvature measurements with a Talyrond revealed a centrally located circumferential groove in the race approximately 0.013 mm (0.0005 inch) deep, Figure 4(a). This groove was not centered on the band of spalling, but did include a portion of it. Apparently it was also primarily the result of wear, similar to the wear bands on the inner race.

Observation of the races by scanning electron microscopy (SEM) revealed the pits to be jagged and steep sided, Figures 5 and 6(b). Such pits on bearing races are characteristic of fatigue spalls.

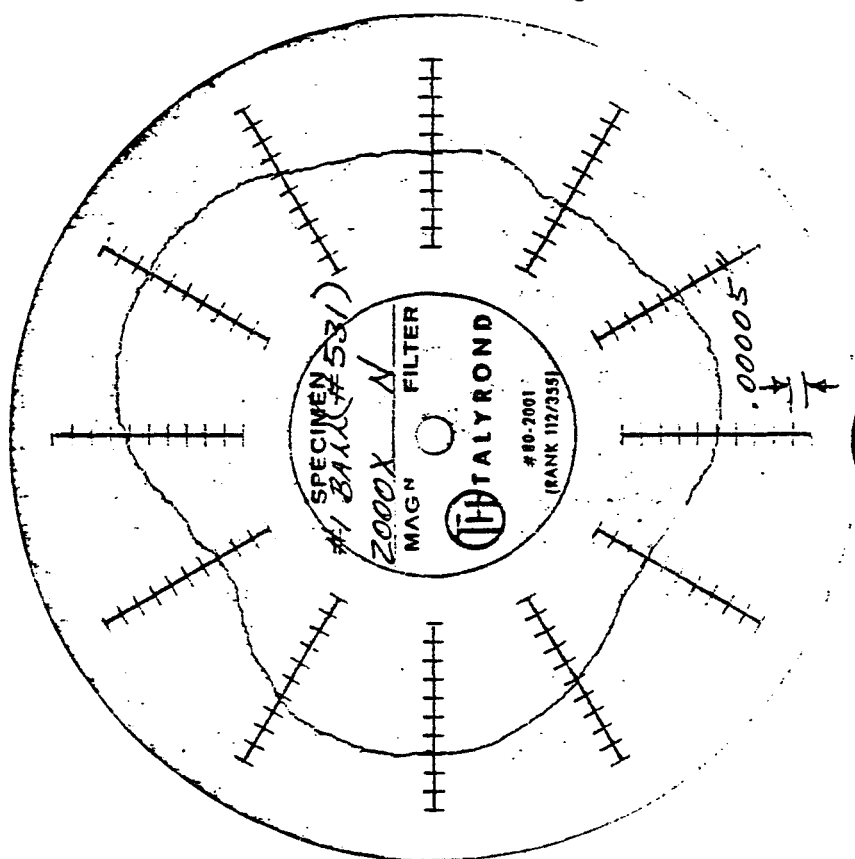


ORIGINAL PAGE IS  
OF POOR QUALITY

FIGURE 3. INNER RACE CROSS-RACE CURVATURES TAKEN AT POSITIONS 180 DEGREES APART  
ON BEARING S/N 8549531. Radial Magnification: 1 division =  
12.7  $\mu$ m (.0005 inch)

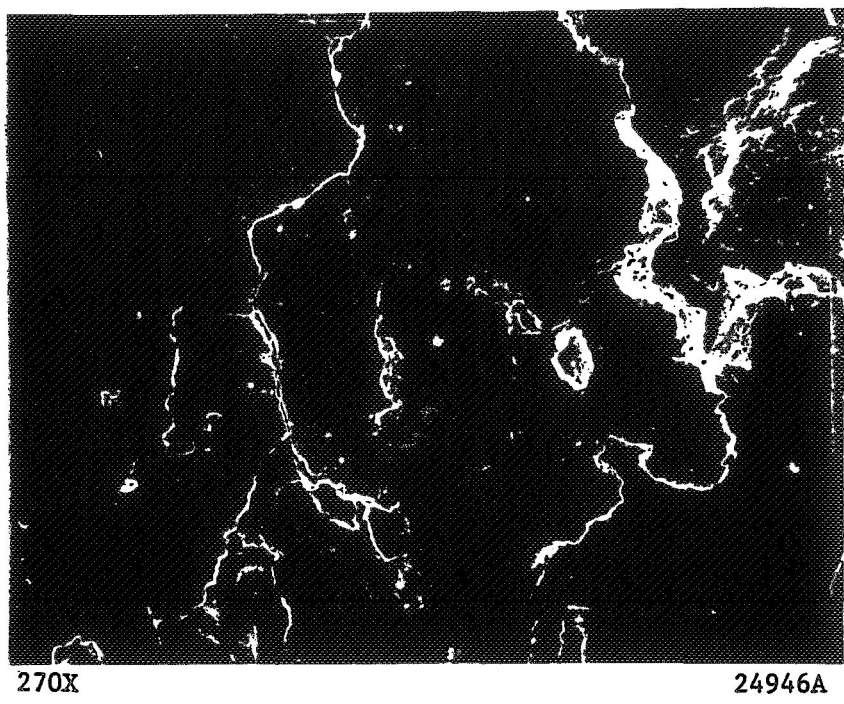


a. Outer Race  
Radial Magnification: 1 division = 6.35  $\mu\text{m}$   
(250 micrometers)



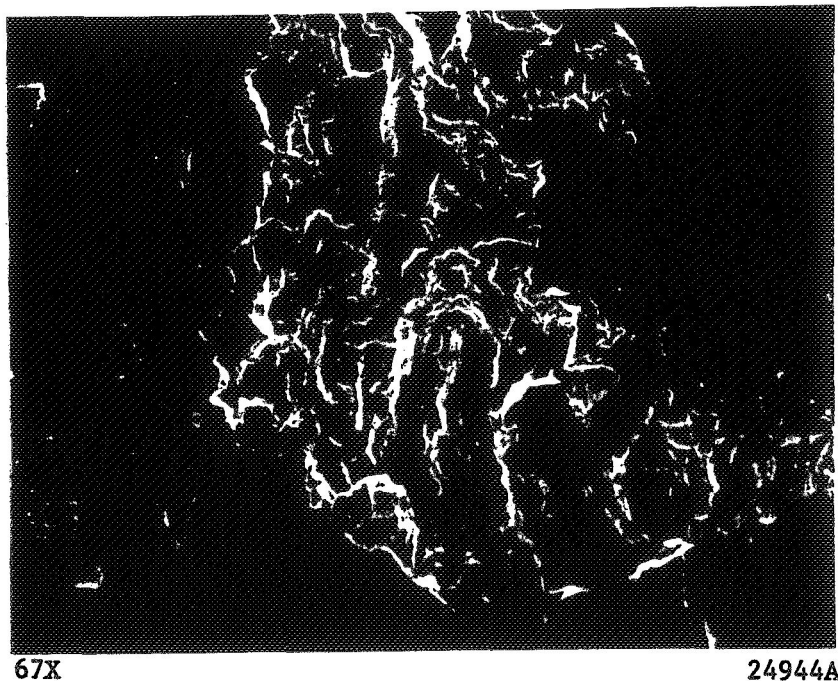
b. Ball  
Radial Magnification: 1 division = 1.27  $\mu\text{m}$   
(50 micrometers)

FIGURE 4. OUTER RACE CROSS-RACE CURVATURE AND TYPICAL NON-SPALLED BALL ROUNDNESS  
FROM BEARING S/N 8549531



270X

24946A

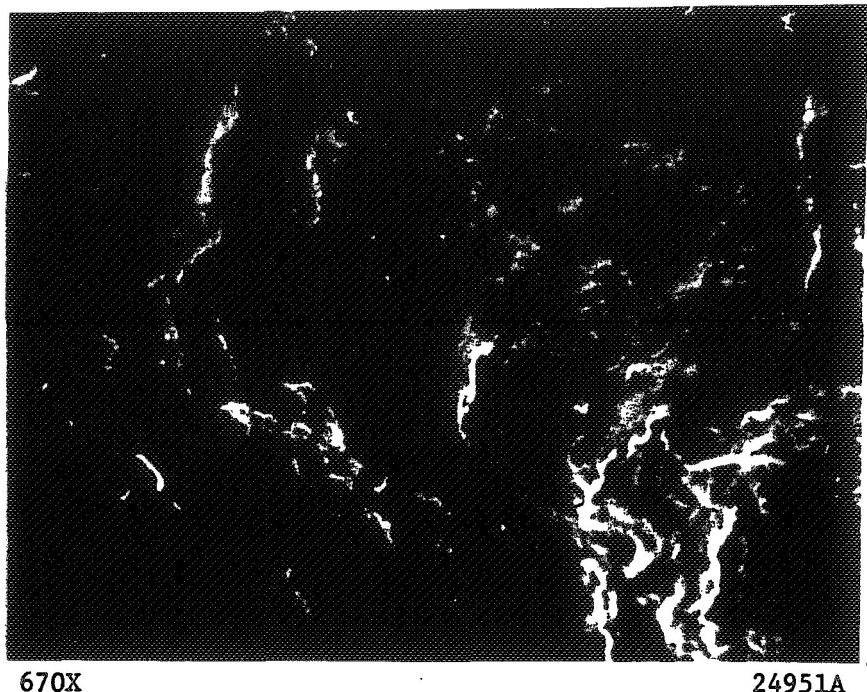


67X

24944A

FIGURE 5. SCANNING ELECTRON MICROGRAPHS OF SURFACE SPALLING ON INNER RACE OF BEARING  
S/N 8519531

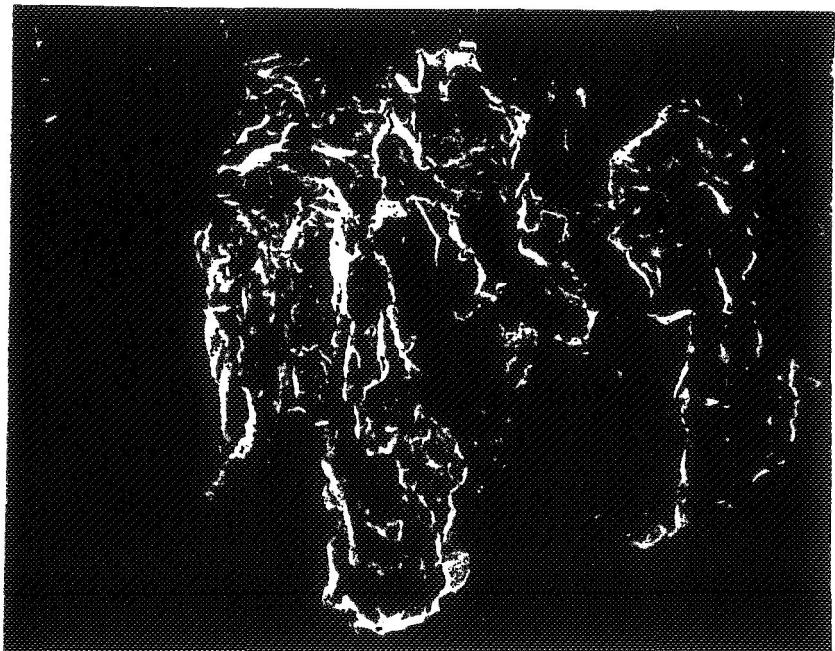
ORIGINAL PAGE IS  
OF POOR QUALITY



670X

24951A

a. Ball



33X

24947A

b. Outer Race

FIGURE 6. SPALLING ON BALL AND OUTER RACE SURFACES  
OF BEARING S/N 8519531

ORIGINAL PAGE IS  
OF POOR QUALITY

Metallographic sections of the races revealed that the subsurface damage was much more extensive than apparent by the spalls at the surfaces. Examples are shown in Figure 7 of the widespread subsurface cracking below the relatively small fatigue pits at the surface. The depth of the major cracks was approximately 0.14 mm (0.005 inch).

At higher magnification, Figure 8, the cracks were found to be oxidized in many areas. Although the bearings operate in a bath of liquid oxygen, no similar oxidation was observed at the free bearing surfaces. Since oxidation at the cracks would seemingly require an elevated temperature, a microhardness traverse was made across the cracked region into the base material. As shown in Table 1, there was no definite trend of low hardness readings to indicate tempering associated with elevated temperatures. The lower readings near the cracks probably resulted from the indentor being too close to the edge to be properly supported.

Examination of the microstructure after etching confirmed the absence of tempering. Possibly the oxide resulted from localized surface heating during repeated applications of rolling contact stress. Any widespread heating of the area would either temper the steel to a lower hardness or would leave a heat-affected zone if it were re-hardened. A heating of the entire race to above critical temperatures would be expected to cause an oxidation of the free surfaces as well. Therefore, if the formation of oxides in the cracks requires an elevated temperature, it was apparently restricted to a very thin depth at the crack surfaces.

#### Balls

Since only half of each race and six of the thirteen balls were supplied for inspection, a complete assessment of the damage could not be made. Of the six balls received, one had a small spalled area, one had a large spalled area, and four were relatively smooth. A spalled region of one of the balls is shown in Figure 6(a), and a Talyrond trace of an unspalled ball is shown in Figure 4(b). Ball damage is expected after race spalling occurs, and the damage observed on the balls was not considered to be extensive in view of the heavy race spalling and wear.

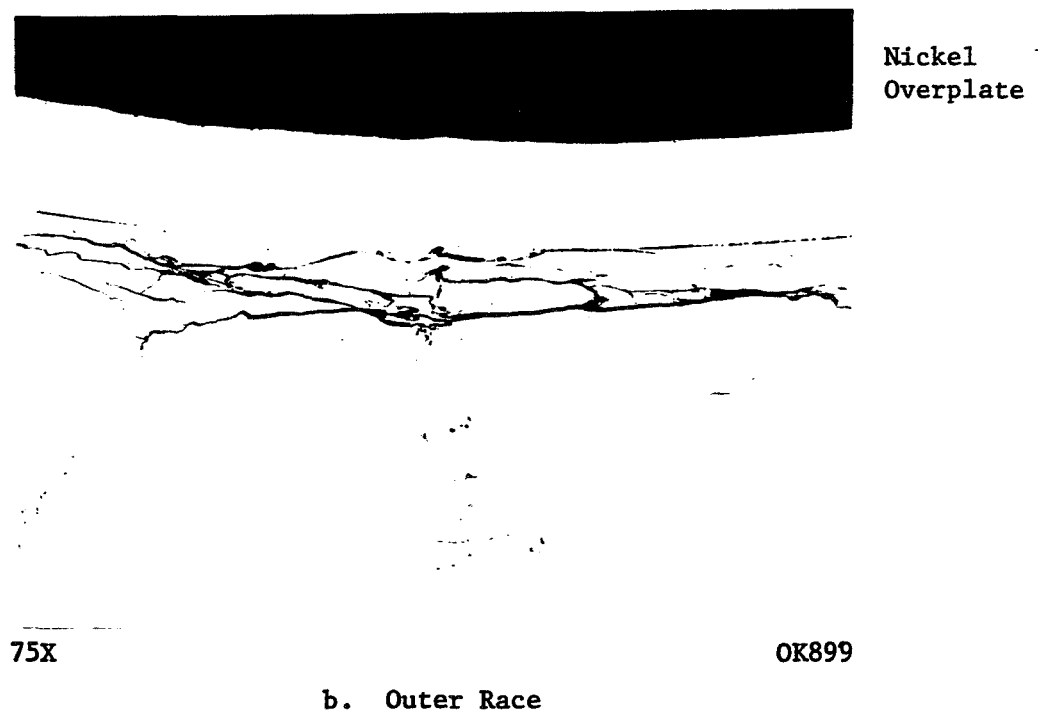
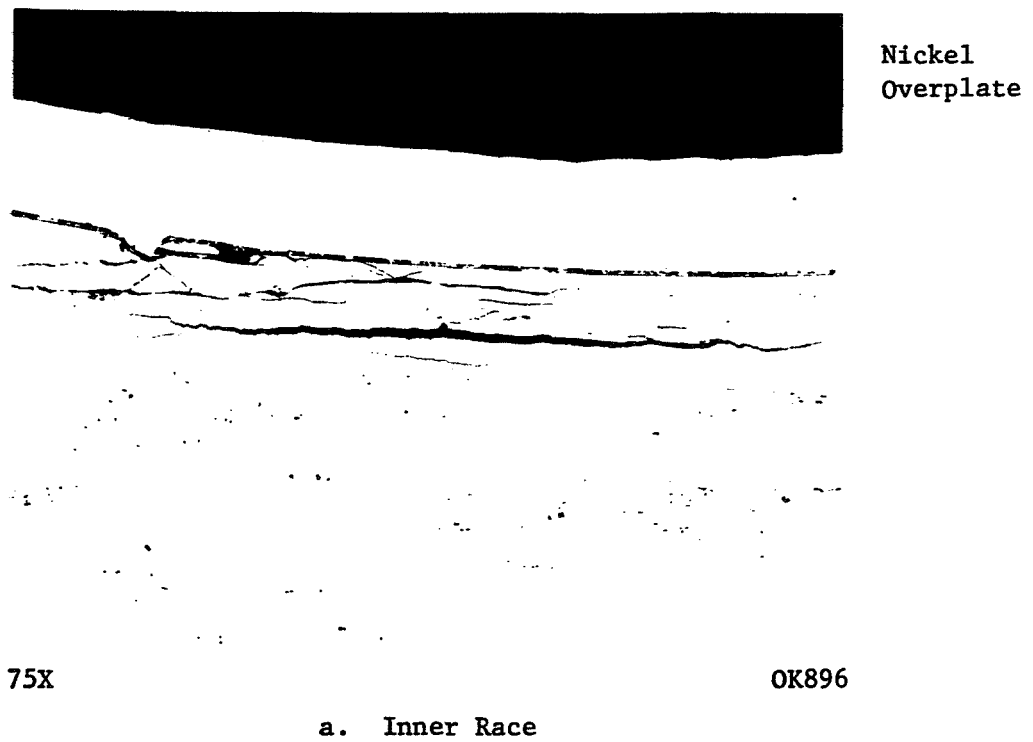


FIGURE 7. SUBSURFACE CRACKING ON RACES OF BEARING S/N 8519531

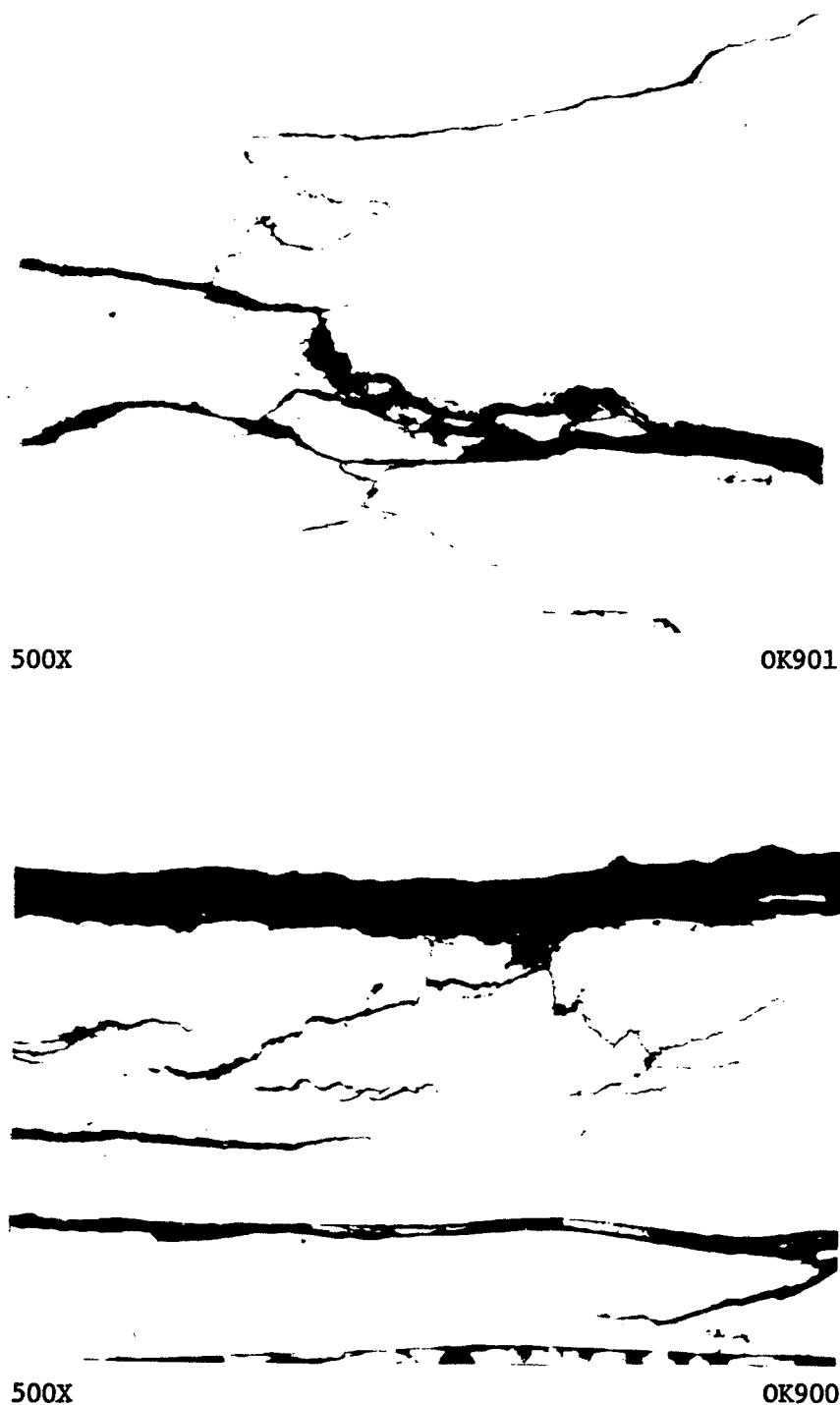


FIGURE 8. OXIDE IN SUBSURFACE CRACKS ON RACES  
OF BEARING S/N 8519531

ORIGINAL PAGE IS  
OF POOR QUALITY

TABLE 1. MICROHARDNESS READINGS TAKEN ACROSS REGION OF  
SUBSURFACE CRACKS ON RACES OF BEARING  
S/N 8519531

Depth Below Surface, <u>mm</u> <u>(inches)</u>	Knoop Hardness Number, 100 g (0.220 pound) load	
	<u>Inner Race</u>	<u>Outer Race</u>
0.025 (0.001)	798	764
0.051 (0.002)	747	764
0.076 (0.003)	544	874
0.102 (0.004)	634	440
0.127 (0.005)	798	874
0.152 (0.006)	798	747
0.17 <sup>f</sup> (0.007)	732	781
0.203 (0.008)	916	855

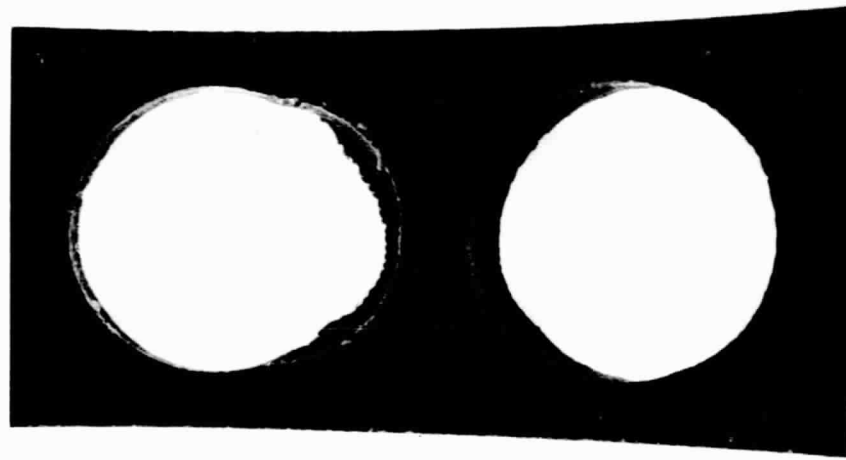
Retainer

The retainer was heavily worn in several pockets as the result of sliding contact with the balls. Figure 9 shows the elongation observed in one of the ball pockets. Measurements of the pocket dimensions are presented in Table 2. The extensive wear experienced by several of the pockets is indicative of high ball-cage loading, which typically occurs in bearings undergoing failure. The retainer damage progresses until the section size is unable to support the ball loads, at which point the retainer fractures and at least major portions are thrown from the bearing. Without a retainer, the balls are free to migrate, shaft location is lost, and rapid extensive secondary damage can be expected.

Bearing S/N 8549515Races

In contrast to bearing S/N 8549531, the mating bearing S/N 8549515 showed evidence of very mild service and no indication of failure being imminent. The inner race had contact paths indicative of a synchronous radial load in addition to the axial load, but was free of obvious wear or spalling. At one extreme, the first ball contact path extended to the chamfer in a very mildly worn band approximately 1.1 mm (0.045 inch) wide. Inward from this band was a polished band 0.64 mm (.025 inch) wide, which was followed by another mildly worn band approximately 3.2 mm (.125 inch) wide. At the other extreme located 180 degrees from the above location, the track was a single mildly worn band 4.1 mm (0.160 inch) wide located with its edge 1.3 mm (0.050 inch) from the chamfer. The ball contact was more clearly defined in this location and became increasingly diffusive as it moved toward its extreme position nearest the chamfer.

The outer race was very mildly worn in a single ball contact path approximately 3.2 mm (0.125 inch) in width and located with one edge 2.9 mm (0.115 inch) from the edge radius. The track had shallow dents, probably from debris, but was uniform in width and location.



3X

OK927

FIGURE 9. BALL POCKET ELONGATED BY WEAR  
IN RETAINER FROM BEARING  
S/N 8519531

ORIGINAL PAGE IS  
OF POOR QUALITY

TABLE 2. BALL POCKET DIMENSIONS ON RETAINER  
FROM BEARING S/N 8519531

Circumferential Direction mm      (inches)	Axial Direction, mm      (inches)	Wear, mm      (inches)
15.8 (0.622)	13.5 (0.533)	2.26 (0.089)
15.3 (0.604)	13.5 (0.531)	1.85 (0.073)
16.4 (0.645)	13.6 (0.534)	2.82 (0.111)
15.8 (0.622)	13.5 (0.533)	2.26 (0.089)
14.4 (0.565)	13.5 (0.531)	0.86 (0.034)
14.5 (0.569)	13.5 (0.533)	0.91 (0.036)
14.7 (0.578)	13.6 (0.534)	1.09 (0.043)
14.2 (0.561)	13.6 (0.534)	0.69 (0.027)
14.4 (0.566)	13.5 (0.533)	0.84 (0.033)
15.0 (0.589)	13.6 (0.532)	0.79 (0.031)
14.3 (0.563)	13.6 (0.534)	0.76 (0.030)
14.8 (0.583)	13.5 (0.533)	1.27 (0.050)

Note: Drawing specification is for round holes  
 13.3 <sup>+0.254</sup> mm (0.525 <sup>+0.010</sup> inch) in diameter.  
<sub>-0.000</sub>      <sub>-0.000</sub>

Talyrond cross-race curvature measurements, shown in Figures 10 and 11(a), confirm the mild and uniform wear. A graphical illustration of the ball contact paths is presented in Figure 14 as part of the load-estimate calculations.

Metallographic sections of the races showed a normal micro-structure for 440C steel and no indications of subsurface damage. Similarly, SEM inspections of the race surfaces confirmed the mild wear and freedom from damage.

#### Balls

The balls had no apparent wear. The only evidence of contact was in the form of mild color bands. The Talyrond trace in Figure 11(b) of a typical ball confirmed the mild wear and demonstrated the excellent conformity to roundness.

#### Retainer

No retainer was received for inspection from bearing S/N 8549515.

### LOAD AND STRESS ANALYSIS

#### General Approach

The bearing inspections have shown not only that extensive fatigue pitting was present, but also that a considerable variation occurred in the location of the ball contact paths in the bearings. Such variations are most likely the result of radial loading due to imbalances in the shaft combined with axial loads of varying magnitude. The purpose of the analysis was to estimate the magnitude of these loads and the bearing stresses associated with these loads.

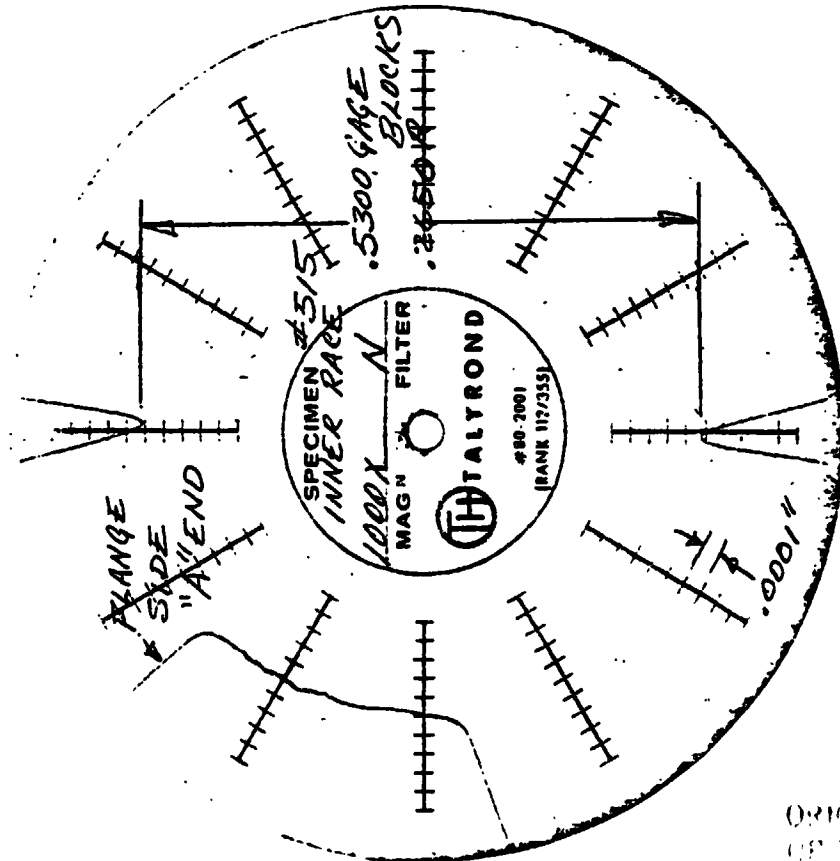
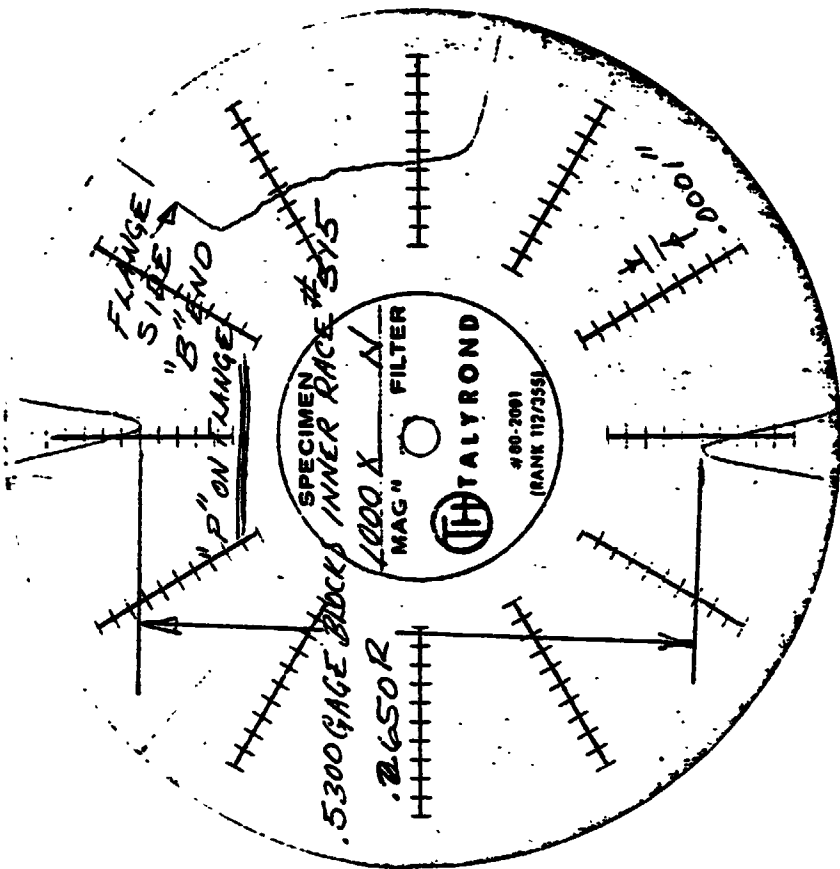
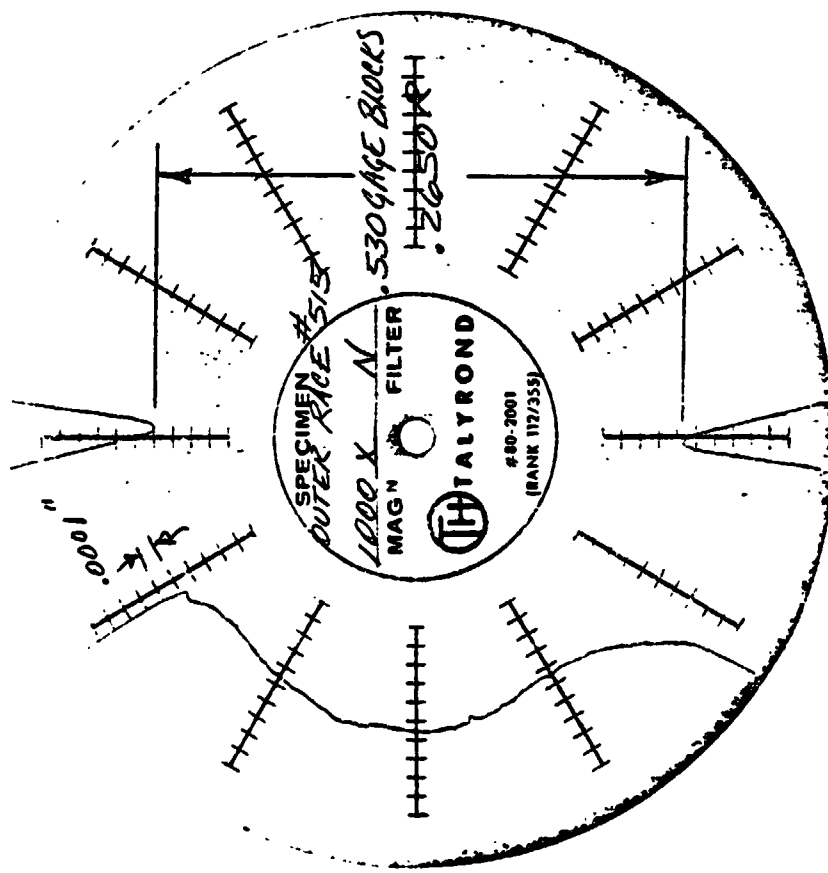
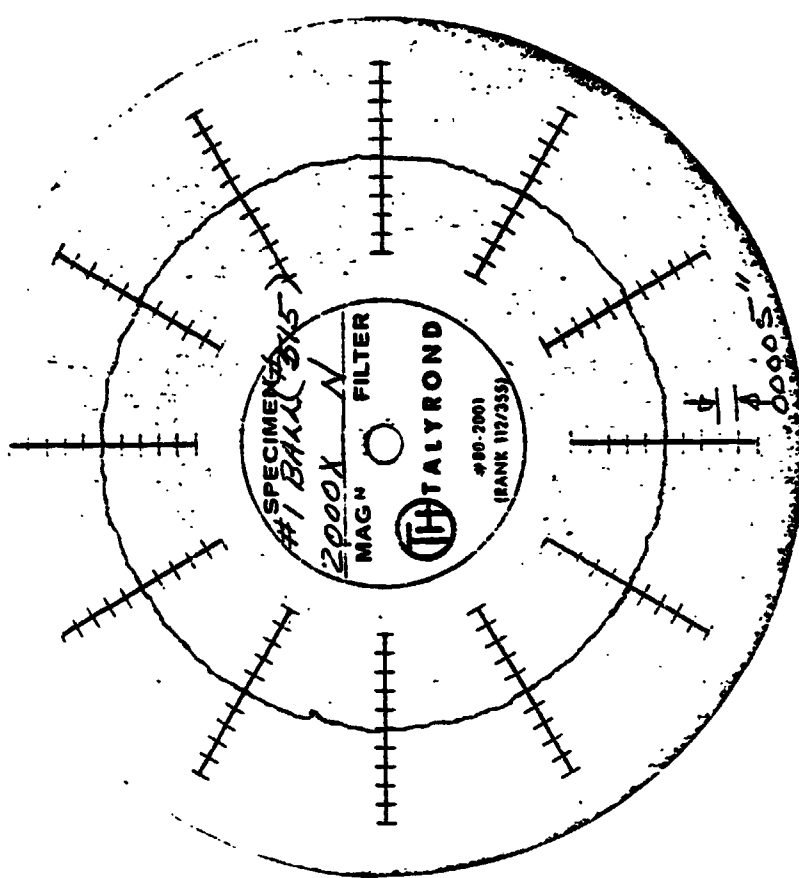


FIGURE 10. INNER RACE CROSS-RACE CURVATURES TAKEN AT POSITIONS 180 DEGREES APART ON BEARING S/N 8549414. Radial Magnification: 1 division = 2.54  $\mu$ m (100 microinches)

ORIGINAL PAGE IS OF POOR QUALITY



a. Outer Race  
Radial Magnification: 1 division = 2.54  $\mu\text{m}$   
(100 microinches)



b. Ball  
Radial Magnification: 1 division = 1.27  $\mu\text{m}$   
(50 microinches)

FIGURE 11. OUTER RACE CROSS-RACE CURVATURE AND TYPICAL BALL ROUNDNESS FROM BEARING S/N 8549515

The method for bearing load computation at Battelle involves the use of a computer program series under the general name, BASDAP. BASDAP programs can be used for static or dynamic analysis of bearings for a wide range of applications. For example, BASDAP programs have been used in:

- (1) Static or quasi-dynamic analyses to determine ball-race stresses and ball steady-state motions
- (2) Determining the effects of unusual load conditions, such as staggered ball spacings
- (3) Analyses of dynamic behavior of the cage to determine cage stability and ball-cage loadings.

The BASDAP program treats each bearing in a set independently.

For the project discussed herein, a quasi-dynamic version of the BASDAP computer code was utilized. This code involves calculation of ball-race forces (inner and outer), contact pressures, contact dimensions, and contact angles as a function of (1) axial load, (2) radial load, and (3) centrifugal load on the bearing.

The computation technique involves first computing the load sharing between the balls in the absence of centrifugal forces. This involves a formalized trial and error (nesting type) procedure. Estimates of the axial and radial deflections of the bearings are made and the correct value of these deflections results in the correct radial and axial load. After the ball load sharing has been computed, the effect of centrifugal forces on contact angle is computed. This force causes the inner and outer race contact angles to be different from each other as well as different from the static contact angles. The method for the deflection and contact angles calculation is modeled after the classic work of A.B. Jones.\*

---

\*Jones, A.B., "A General Theory for Elastically Constrained Ball and Roller Bearings Under Auxiliary Load and Speed Conditions", Trans. ASME, J. Basic Eng., Vol. 82, Ser. D., No. 2, June 1960, pp 309-320.

Inputs for Bearing Load Calculations

The BASDAP computer calculations were made for the bearing specifications provided in Print 007955. The primary inputs of interest were:

Radius of Pitch : 1.595 inches (.041 mm)  
Ball Radius : 0.25 inch (.00636 mm)  
Contact Angle : 20.5 degrees  
Number of Balls : 13  
Speed : 30,000 rpm  
  
Inner and Outer Race  
Curvature : 0.53  
  
Axial Load : 3800, 8900, 17,800, 26,700, 35,600 500,  
and 53,400 N (850, 2000, 4000, 6000 ..00,  
10,000, and 12,000 pounds respectively) at  
zero radial load  
  
Radial Load : 8900, 13,300, 17,800, 26,700, 35,600, 44,500,  
and 53,400 N (2000, 3000, 4000, 6000, 8000,  
11,000, and 12,000 pounds respectively) at  
3800 N (850 pounds) axial load.

Estimation of Actual Loads and Fatigue Lives

The measurements made during the bearing inspection of the location and width of the ball contact paths are presented graphically in Figures 12, 13, and 14. An estimation of the loads responsible for these paths was made by a series of BASDAP calculations. By graphical iteration, the load was chosen that gave the best simultaneous fit for both races of contact angle and race contact width. The contact conditions resulting from these loads are also shown in Figures, 12, 13, and 14. Bearing S/N 8549531 was apparently subjected to at least two major load conditions. The first, shown in Figure 12, was a high axial load of approximately 44,500 N (10,000 pounds). This load is responsible for the heavy wear and deformation of the inner race near the race shoulder.

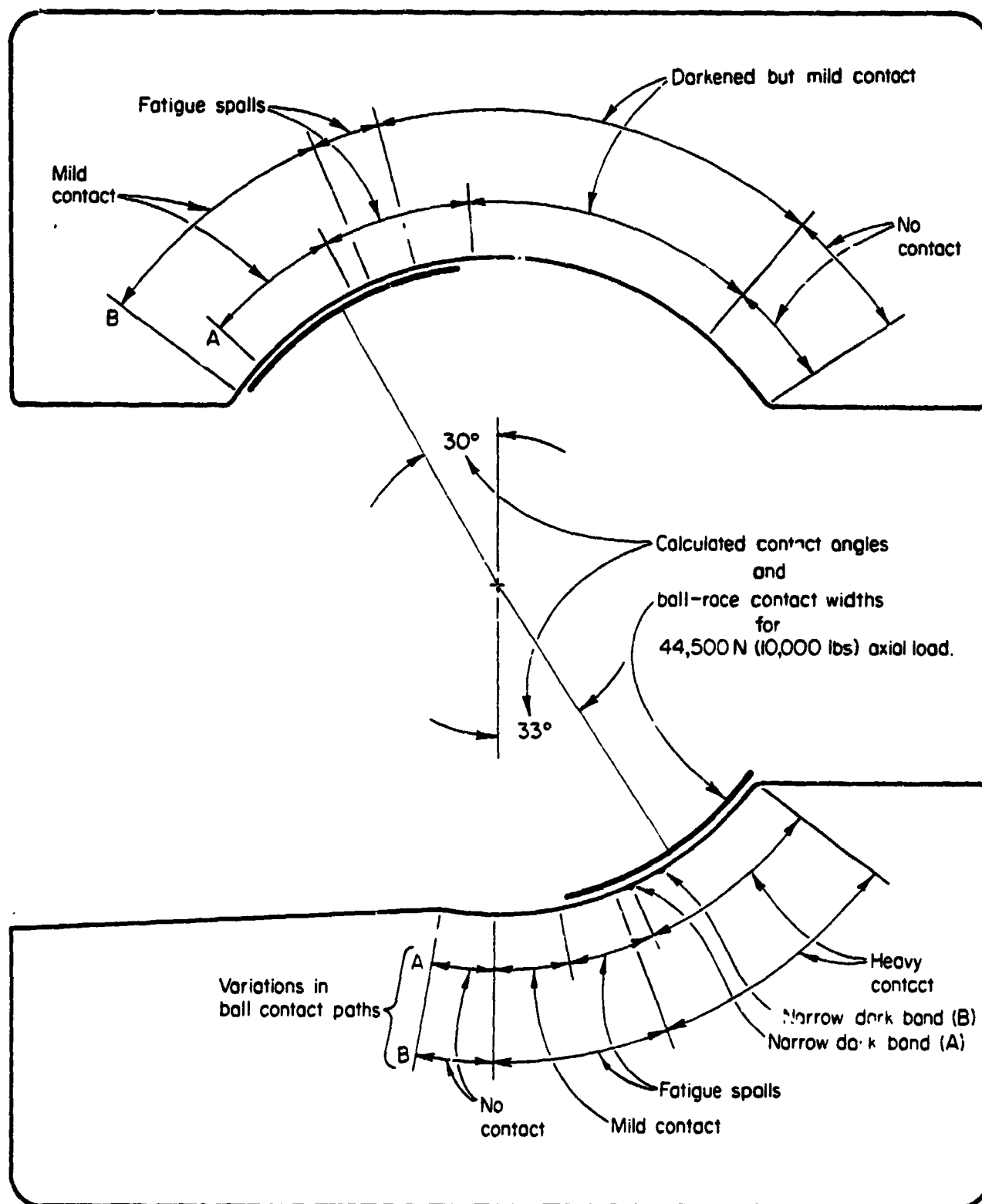


FIGURE 12. LOCATION OF MEASURED BALL CONTACT PATHS ON BEARING S/N 8549531. CALCULATED CONTACT POSITIONS FOR A 44,500 N (10,000 POUNDS) AXIAL LOAD. (Positions "A" and "B" refer to location of extreme positions of ball contact paths.)

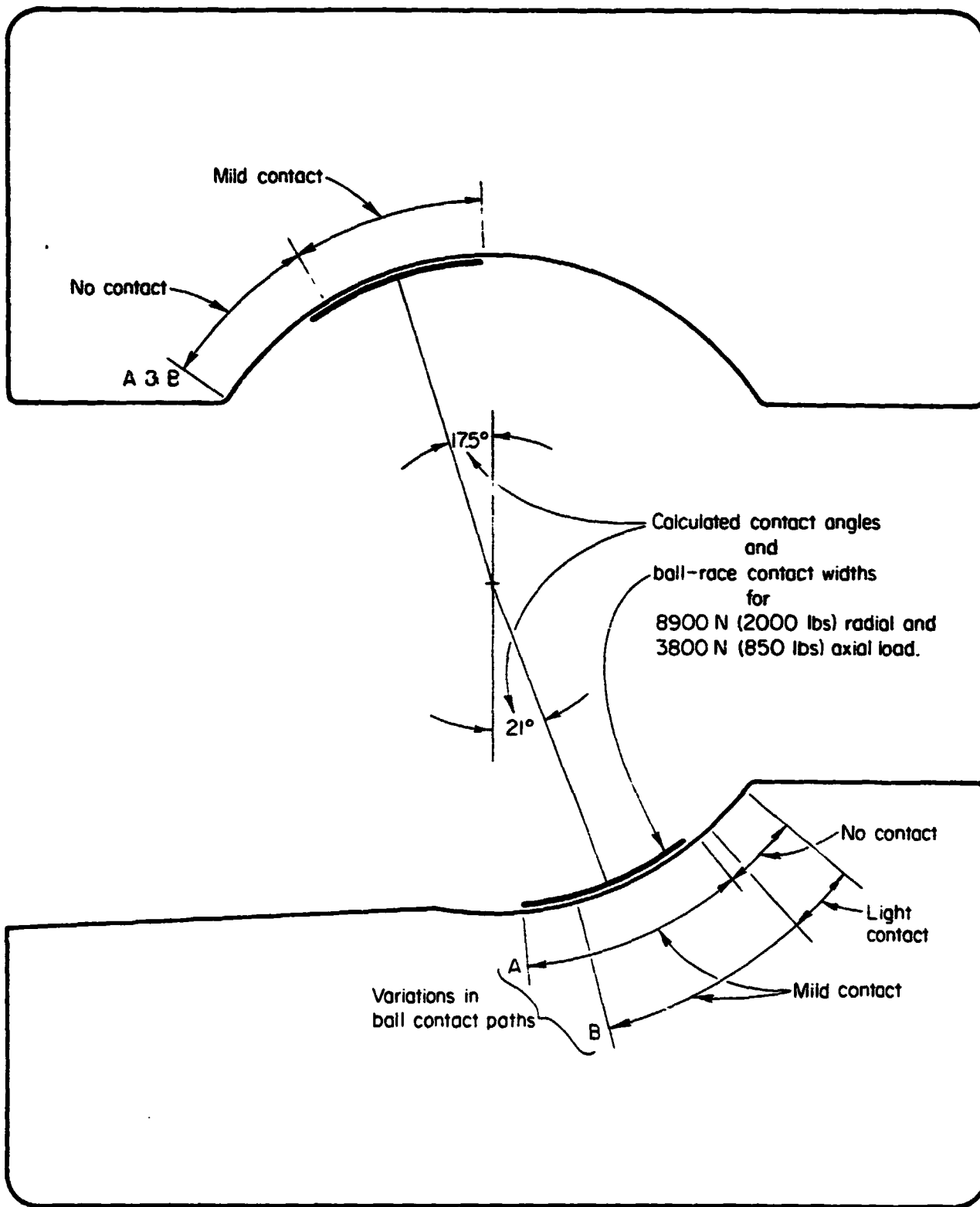


FIGURE 13. LOCATION OF MEASURED P.M. CONTACT PATHS ON BEARING S/N 8549531. CALCULATED CONTACT POSITIONS FOR AN 8900 N (2000 POUNDS) RADIAL LOAD COMBINED WITH A 3800 N (850 POUNDS) AXIAL LOAD. (Position "A" and "B" refer to locations of ball and contact paths)

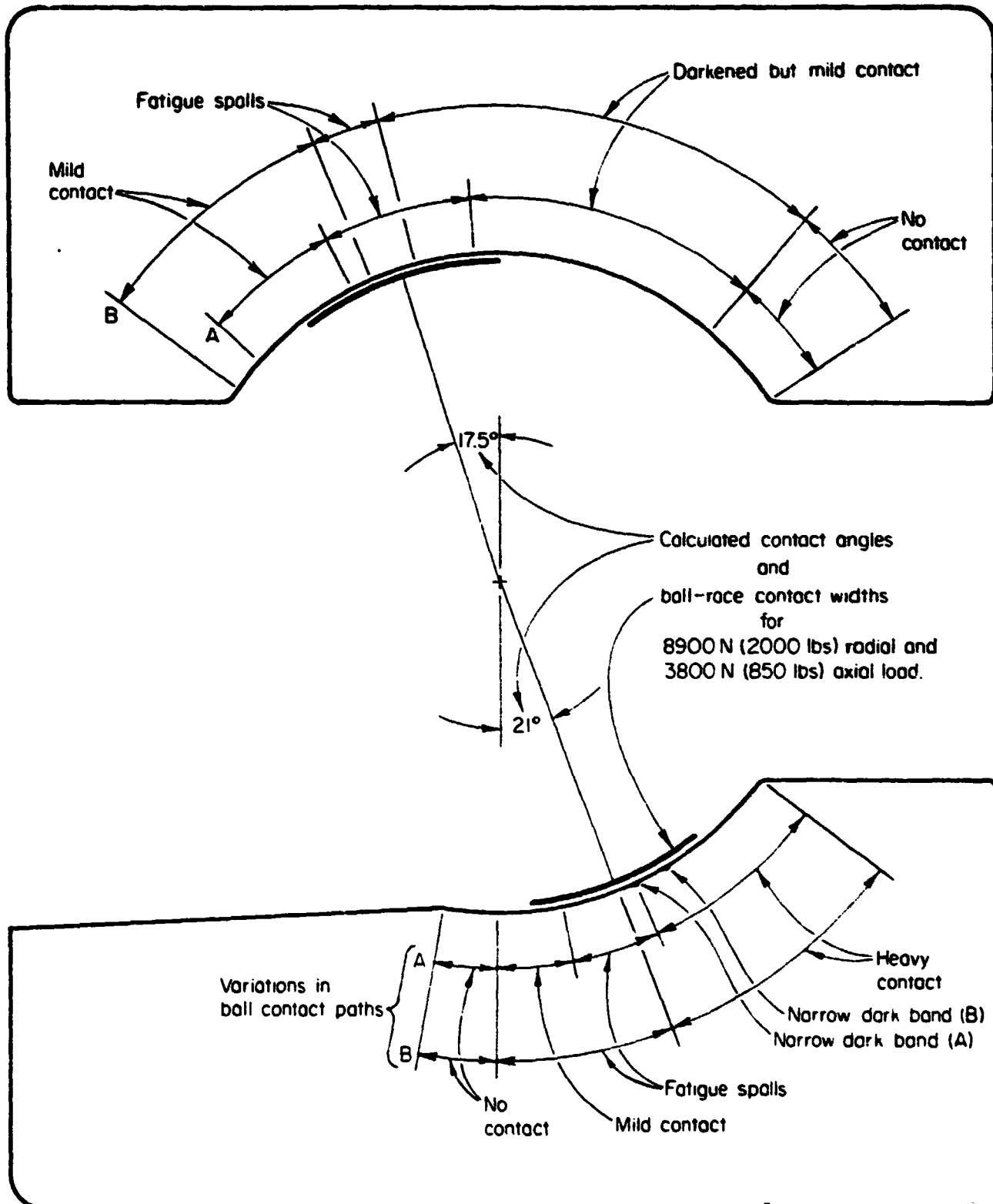


FIGURE 14. LOCATION OF MEASURED BALL CONTACT PATHS ON BEARING S/N 8549515. CALCULATED CONTACT POSITION FOR AN 8900 N (2000 POUNDS) RADIAL LOAD COMBINED WITH A 3800 N (850 POUNDS) AXIAL LOAD. (Positions "A" and "B" refer to location of extreme positions of ball contact paths.)

The second loading condition, shown in Figure 13, consisted of an 8900 N (2000 pounds) radial load combined with a 3800 N (850 pounds) axial load. Since the contact paths from these two load conditions overlap at the location of the fatigue spalls, both loading conditions probably contributed to the fatigue failure. Intermediate loading conditions between those shown in Figures 12 and 13 may also have been applied to the bearing, but the overlapping contact paths do not permit a positive assessment of the possibility. The contact paths on bearing S/N 8549515 are best explained by a radial load of 8900 N (2000 pounds) combined with an axial load of 3800 N (850 pounds), as shown in Figure 14.

Predictions of the effects of various bearing loads on contact stresses and  $B_1$  fatigue life are shown in Table 3. Note that for design conditions, the bearing axial load is 3800 N (850 pounds) with only a slight radial load. For this condition, the bearing should operate for a long period of time if the lubrication is adequate. However, if a 8900 N (2000 pounds) radial load is imposed on the bearing, the life is drastically reduced to 1440-7920 seconds. Likewise, an axial load of 44,500 N (10,000 pounds) reduces the  $B_1$  life to approximately 18-100 seconds. The range of time is based on some uncertainties in the "critical" stress computations. The best estimate is probably midrange between these two extremes. In any case, the high radial load of 8900 N (2000 pounds) or high axial load of 44,500 N (10,000 pounds) is sufficient to cause fatigue spalling in the bearing long before the design time specifications.

Fatigue life is heavily related to the shear stresses generated beneath the bearing surfaces. This shear stress reaches a maximum at a depth of 0.5 times the half-width of the ball-race contact region. For the 44,500 N (10,000 pounds) condition, this depth is about 0.16 mm (0.007 inch), while for the condition of 3800 N (850 pounds) axial load combined with 8900 N (2000 pounds) radial load, this depth is about 0.13 mm (0.005 inch). A section photomicrograph for the bearing S/N 8549531 presumed to have experienced this load is given in Figure 7. The maximum crack depth from this Figure was 0.13 mm (0.005 inch), which correlates quite well with the

TABLE 3. SUMMARY OF BEARING STRESS COMPUTATIONS

Axial Load , N/pounds	Radial Load , N/pounds	Maximum Stress , GPa/ksf	Depth of Maximum Shear Stress , mm/inches	B <sub>1</sub> Life Estimate (a) , seconds
3,800/850 (Design Load)	0 (Design Load)	1.76/250	.074/.0029	24,000 - 130,000
3,800/850	8,900/2,000	2.81/399	.127/.005	1440 - 7920
3,800/850	13,300/3,000	3.34/475	.15 /.006	360 - 2000
44,500/10,000	0	3.73/530	.16 / .0065	29 - 157
53,400/12,000	0	3.94/557	.19 / .0073	18 - 102

(a) Note: Range indicates uncertainties in critical stress computations.

predictions. Continued operation on this bearing would lead to massive removal of race material from this cracked region. These cracks would doubtless be the source of advanced failure of the bearing.

Underlying all of the life computations is the presumption that some minimal level of lubrication is present. If lubrication is insufficient, bearing life can be reduced to an estimated 20 percent of the theoretical life. Therefore, it is mandatory that proper attention be given to both lubrication and to bearing load if the bearings are to withstand the Shuttle operation. Since the turbopump bearings are lubricated by a transfer film mechanism of unknown reliability having limitations on permissible contact stresses, the  $F_1$  fatigue life predictions may actually be optimistic. This further emphasizes the critical need for reducing the applied loads to acceptable levels.

#### Measuring Units

Since the bearing drawing and all input data provided by NASA were in English units, all measurements and calculations were performed in English units. Therefore, the SI units presented in this report were converted from English units. Data on which this report is based are located in Battelle Laboratory Record Book No. 34405.